Relic density, WIMP miracle and thermal DM generation

Temperature fluctuations in the CMB

CMB are photons that decoupled from the thermal bath. The surface of last scattering is the one defined by the photons that could come freely to reach us today.

$$T_0 = (2.72548 \pm 0.00057)$$

The value of the variations is of the order $\delta T / T \leq 10^{-5}$ in the sphere of last scattering. If we study these variations in detail we can understand better the temperature fluctuations at that time. Temperature fluctuations on the sphere can be described via spherical harmonics, with the usual polar and azimuthal angles

$$\frac{\delta T(\theta, \phi)}{T_0} = \frac{T(\theta, \phi) - T_0}{T_0} = \sum_{l=0}^{\infty} \sum_{m=-l}^{l} a_{lm} Y_{ml}(\theta, \phi)$$

In order to analyse temperature fluctuations, the relevant measure is the variance of the temperature distribution

$$\frac{1}{4\pi} \int d\Omega \left(\frac{\delta T(\theta, \phi)}{T_0} \right)^2 = \frac{1}{4\pi} \sum_{m,l} |a_{lm}|^2$$

Temperature fluctuations in the CMB

The index m describes the angular momentum in a particular direction, but because there is no special direction in the sphere of last scattering the a_{lm} coefficients do not depend on m. Thus, the sum over m yields 2l+1 identical terms. The average of $|a_{lm}|^2$ over m will be defined as the observed power spectrum

$$C_l = \frac{1}{2l+1} \sum_{m=-l} |a_{lm}|^2$$

The values of the coefficients C_l can be determined using

$$\frac{1}{4\pi} \int d\Omega \left(\frac{\delta T(\theta, \phi)}{T_0} \right)^2 = \frac{1}{4\pi} \sum_{l=0}^{\infty} \frac{2l+1}{4\pi} C_l$$

Temperature fluctuations measured by PLANCK allows to calculate C_l.

The peaks are generated by acoustic oscillations which occur in the baryon-photon fluid at the time of photon decoupling.

Regions with a large accumulation of DM form gravitational wells, which pull the baryon-photon fluid inside it resulting in a compression of the fluid.

At the same time the relativistic photons exert a pressure that counteracts the gravitational pull, which results in a rarefaction of the fluid.
These counteracting forces create oscillations in the baryon-photon fluid and lead to temperature fluctuations in the photon spectrum during decoupling.

Temperature fluctuations in the CMB

The odd numbered peaks correspond to the decoupling of photons during a compression phase, while even numbered peaks correspond to a decoupling during a rarefaction phase.

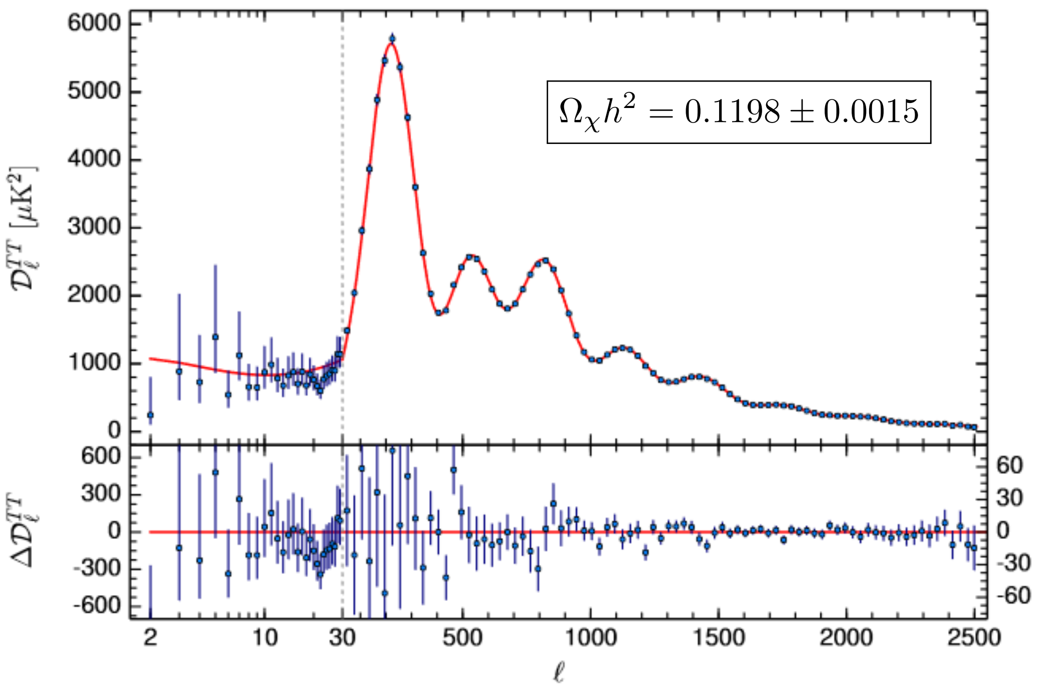

To fit the data points given in a model with 6 independent cosmological parameters is used under the assumption of a flat universe. This model is referred to as the "base ΛCDM", which includes the Hubble constant H , and the baryon and DM fraction

The first peak corresponds to the time of last scattering where the fluid compressed once. Determining its position gives information about the curvature of the universe.

The second peak corresponds to one compression and one rarefaction of the fluid. A large relative baryon content in the baryon-photon fluid would lead to an increase in amplitude of the compression peaks and at the same time to a decrease of the rarefaction peaks. Therefore, by measuring the ratio between the first and the second peak, the baryon content of the universe can be obtained.

The height of the third peak determines the amount of DM in the universe. Since, DM does not interact with photons, it only contributes to the strength of the compression peaks. Therefore, a large third peak is a sign of a sizeable DM component in the universe.

Mechanisms of thermal DM generation - freeze-out

The relic density is calculated using the Boltzmann equation which describes the change of a number density $n(t)$ with time. If $a(t)$ is the linear dimension of the universe,

$$0 = \frac{d}{dt}[n(t)\,a(t)^3] = \dot{n}(t)a(t)^3 + 3n(t)a(t)^2\dot{a}(t) \quad \Rightarrow \quad \dot{n}(t) + 3H(t)\,n(t) = 0$$

Where H is the Hubble constant. This would be the equation that would hold if the density of all particles would be constant with time. The evolution of the density of DM is also related to the production or annihilation of DM

$$\dot{n}(t) = -\,3H(t)n(t) - <\sigma v>_{\chi\chi} (n^2(t) - n_{eq}^2)$$

where $<\sigma v>_{\chi\chi}$ is the thermal averaged cross section (luminosity), and n_{eq} is the equilibrium density. Note that

$$[\sigma v n] = m^2 \frac{m}{s}\frac{1}{m^3} = \frac{1}{s}$$

The thermal averaged cross section is given by

$$<\sigma v>_{\chi\chi} = \frac{\int d^3p_{\chi,1}\int d^3p_{\chi,2}\, e^{-(E_{\chi,1}+E_{\chi,2})/T}\ \sigma_{\chi\chi}v}{\int d^3p_{\chi,1}\int d^3p_{\chi,2}\, e^{-(E_{\chi,1}+E_{\chi,2})/T}} \qquad v = \frac{\sqrt{(p_{\chi,1}\,p_{\chi,2}) - m_\chi^4}}{E_{\chi,1}\,E_{\chi,2}}$$

Mechanisms of thermal DM generation - freeze-out

The equation is usually simplified with a change of variables $Y = ns$, leading to

$$\frac{dY}{dx} = -\sqrt{\frac{\pi}{45G}}\frac{g_*^{1/2}m_\chi}{x^2}\langle\sigma v\rangle_{\chi\chi}(Y^2 - Y_{\rm eq}^2)$$

Where $x = m_\chi/T$, G is the gravitational constant and g_* are the relativistic degrees of freedom (that evolve over time). We have assumed that the total entropy on the universe remains constant with time.

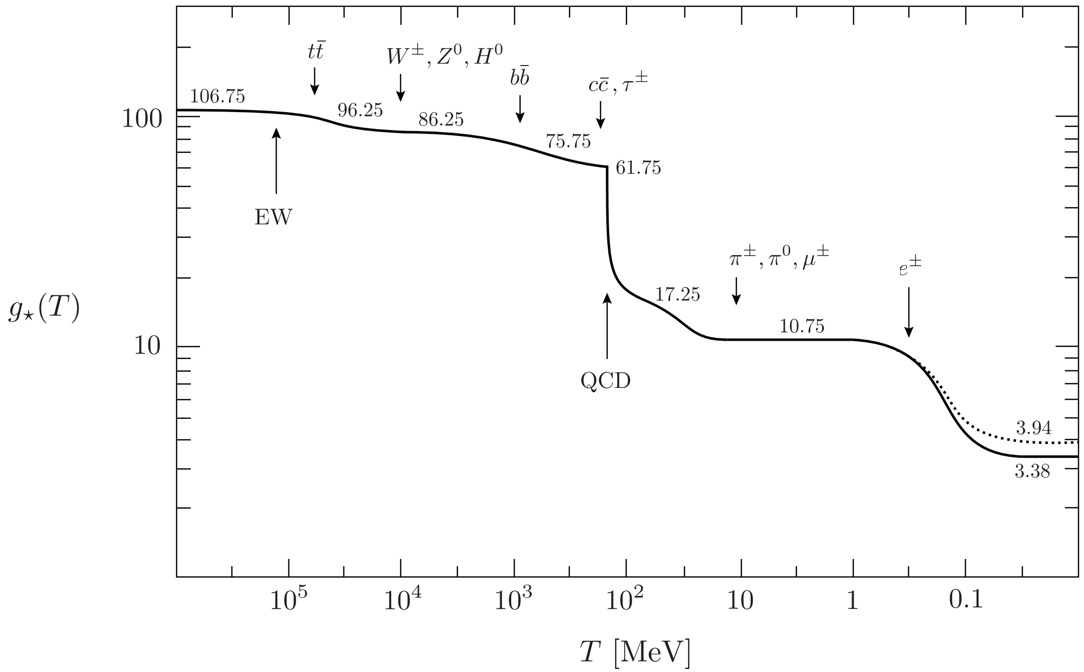

Figure 3.4: *Evolution of relativistic degrees of freedom $g_\star(T)$ assuming the Standard Model particle content. The dotted line stands for the number of effective degrees of freedom in entropy $g_{\star S}(T)$.*

$g_b = 28$ photons (2), $W^\pm$ and Z^0 $(3 \cdot 3)$, gluons $(8 \cdot 2)$, and Higgs (1)

$g_f = 90$ quarks $(6 \cdot 12)$, charged leptons $(3 \cdot 4)$, and neutrinos $(3 \cdot 2)$

$$g_\star = g_b + \frac{7}{8}g_f = 106.75$$

Mechanisms of thermal DM generation - freeze-out

Going back to the Boltzmann equation in the form

$$\frac{dY}{dx} = -\sqrt{\frac{\pi}{45G}}\frac{g_*^{1/2}m_\chi}{x^2}\langle\sigma v\rangle_{\chi\chi}(Y^2 - Y_{\rm eq}^2) \qquad s' = h_{\rm eff}(T)\frac{2\pi^2}{45}T^3 \quad , \quad \rho = g_{\rm eff}(T)\frac{\pi^2}{30}T^4$$

We can now integrate the equation to get the value of the Yield today.

The relic density can be calculated via

$$\Omega_\chi = \frac{\rho_{\chi,0}}{\rho_{\rm c}} = \frac{m_\chi n_0}{\rho_{\rm c}} = \frac{m_\chi s_0 Y_0}{\rho_{\rm c}}$$

where s_0 is the entropy density today and $\rho_c = 3H^2/(8\pi G)$ is the critical density that separates a expanding from a collapsing universe. To match the definition of the observed relic density we need to multiply the above equation by

$$h^2 = \left(\frac{H}{100\,\frac{\rm km}{\rm s\,Mpc}}\right)^2$$

Introducing numerical values we get the following expression

$$\Omega_\chi h^2 = m_\chi s_0 Y_o \frac{8\pi G}{3H^2} \approx 2.742 \times 10^8 \frac{m_\chi}{GeV} Y_0$$

Experimental value

$$\Omega_\chi h^2 = 0.1198 \pm 0.0015$$

Now we just need to calculate Y_0. And we start with our favourite model

$$V = \mu^2 \Phi^\dagger \Phi + \lambda \left(\Phi^\dagger \Phi\right)^2 + \mu_S^2 \Phi_S^2 + \lambda_S \Phi_S^4 + \lambda_3 \Phi^\dagger \Phi \Phi_S^2$$

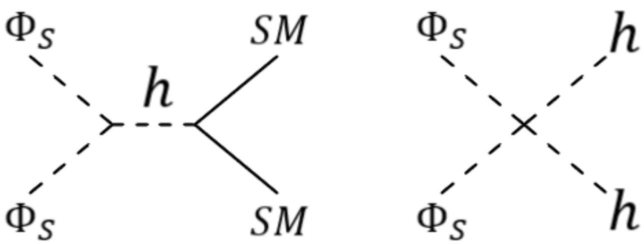

Note that the notation keeps changing!

We need to calculate the cross section for all possible processes, multiply by the relative velocity and find the thermal average.

But before that, the WIMP miracle.

The WIMP miracle

We assume that DM is in thermal equilibrium with the SM particles, and is able to annihilate. At the point of thermal decoupling DM freezes-out with a density that is approximate the one that we measure today. The process of annihilation is

$$\chi\chi \to SM\, SM$$

The interaction rate corresponding to the scattering process just compensates the increasing scale factor at the point of decoupling

$$\Gamma(T_{dec}) = H(T_{dec})$$

If we assume that the interaction rate is set by the electroweak interactions and use the Z-boson coupling and mass, the cross section of the above process is of the order

$$\sigma_{\chi\chi} = \frac{\pi\alpha^2 m_\chi^2}{c_w^2 m_Z^4}$$

And after assuming a lot of other stuff (that could change the order of magnitude but not by much) we reach the conclusion

$$\boxed{\Omega_\chi h^2 \approx 0.12 \left(\frac{13\ \mathrm{GeV}}{m_\chi}\right)^2} .$$

known as the WIMP miracle.

Mechanisms of thermal DM generation - freeze-out

Scalar - The SM is extended by an extra real scalar singlet S, with a Z_2 symmetry $S \to -S$

$$\mathscr{L} = \mathscr{L}_{SM} + \frac{1}{2}(\partial_\mu S)(\partial^\mu S) - V_N + V_{SM}$$

Let us consider the solution (for the minimum) $S = 0;\ h^2 = -\mu^2/(2\lambda);$

And now let us calculate a specific process of DM annihilation to a b-quark pair

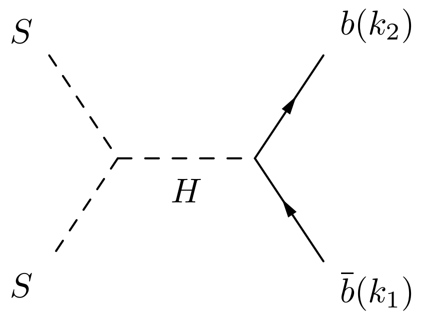

First we calculate the cross section. After that we make an approximation of averaging over a constant. Then we calculate Y today by approximating whatever we can to constants.

What do we need?

$$v = 2\sqrt{\frac{s}{4m_\chi^2} - 1} \qquad \Omega_\chi h^2 = m_\chi s_0 Y_o \frac{8\pi G}{3H^2} \approx 2.742 \times 10^8 \frac{m_\chi}{GeV} Y_0 \qquad m_P = \sqrt{\frac{hc}{2\pi G}} = 1.22 \times 10^{19}\, GeV$$

Mechanisms of thermal DM generation - freeze-out

Now we integrate from x_f (at freeze-out) to infinity

$$\frac{dY}{dx} = -\lambda \frac{Y^2}{x^2} \qquad x = \frac{m_\chi}{T} \qquad \lambda = \sqrt{\frac{\pi}{45G}} g_*^{1/2} m_\chi < \sigma v >_{\chi\chi}$$

The result is

$$Y_0 = Y_\infty \approx \frac{x_f}{\lambda}$$

Considering x_f = 10 calculate the coupling for a DM of 100 GeV.

$$\Omega_\chi h^2 = m_\chi s_0 Y_o \frac{8\pi G}{3H^2} \approx 2.742 \times 10^8 \frac{m_\chi}{GeV} Y_0$$

Mechanisms of thermal DM generation - freeze-out

Back to the complex singlet and considering only the final state with b quarks

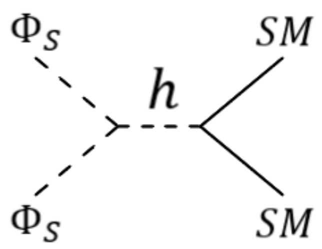

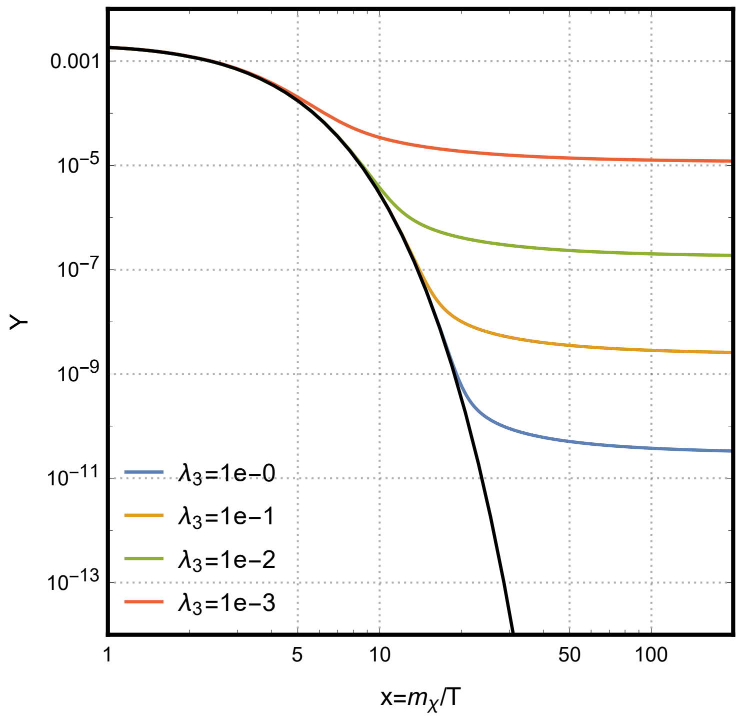

$$\Omega_\chi h^2 = m_\chi s_0 Y_0 \frac{8\pi G}{3H^2} h^2 \approx 2.742 \cdot 10^8 \frac{m_\chi}{\mathrm{GeV}} Y_0$$

The figure shows the evolution of $Y(x)$ as a function of x for different cross sections, that is, for different portal couplings. The larger the coupling the smaller the yield. The reason is that the thermal averaged cross section is a measure of how strongly the SM and the DM bath are coupled. A larger coupling means a more efficient interaction rate. This in turn means a smaller temperature and a larger x.

Mechanisms of DM generation - freeze-in

Freeze-out may not happen if the portal coupling is too small. In that case the DM annihilation channels are not efficient enough to produce the current relic density.

In this regime of very weakly interacting massive particles, also called Feebly Interacting Massive Particles (FIMPs) the mechanism of freeze-in may come to the rescue.

In contrast to freeze- out, the DM particles do not start in thermal equilibrium with the SM and have a low initial abundance. Processes favour the direction of DM production from SM particles instead of annihilation of DM particles into SM particles.

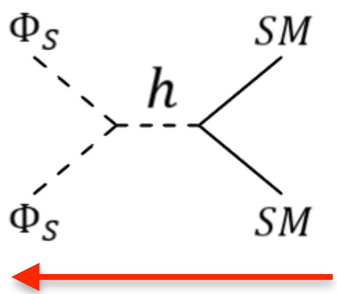

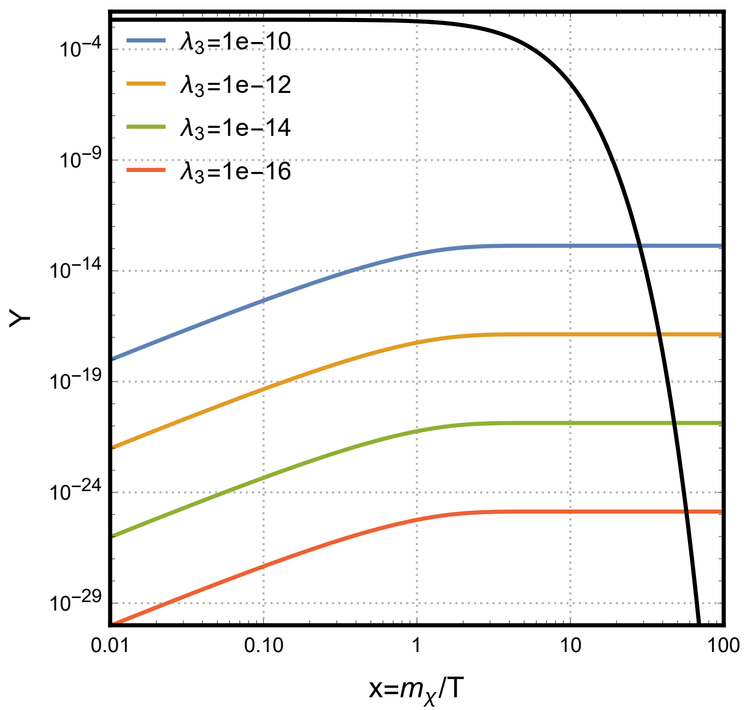

This production happens until the SM coupling to DM is too small to accommodate for the expansion of the universe.

Mechanisms of thermal DM generation - freeze-in

The calculation of the relic density via freeze-in is in general more involved than for freeze-out. Due to the fact that during freeze-in the DM particles are not in thermal equilibrium with the SM particles, the newly produced heavy DM particles have in general less kinetic energy than at equilibrium.

In terms of Y and x the Boltzmann equation now is

$$\frac{dY}{dx} = \sqrt{\frac{\pi}{45G}} \frac{g_*^{1/2} m_\chi}{x^2} \sum_{i,j=1}^{N} \langle \sigma v \rangle_{ij} (Y_{i,eq} Y_{j,eq} - Y_i Y_j)$$

The figure shows the relation between the coupling λ_3 from the potential and the evolution of Y. As for to freeze-out a higher value of λ_3 results in a larger TAC. In contrast to freeze-out though, a larger TAC results in a larger yield (and therefore relic density), because the annihilation of SM particles into DM is more efficient.

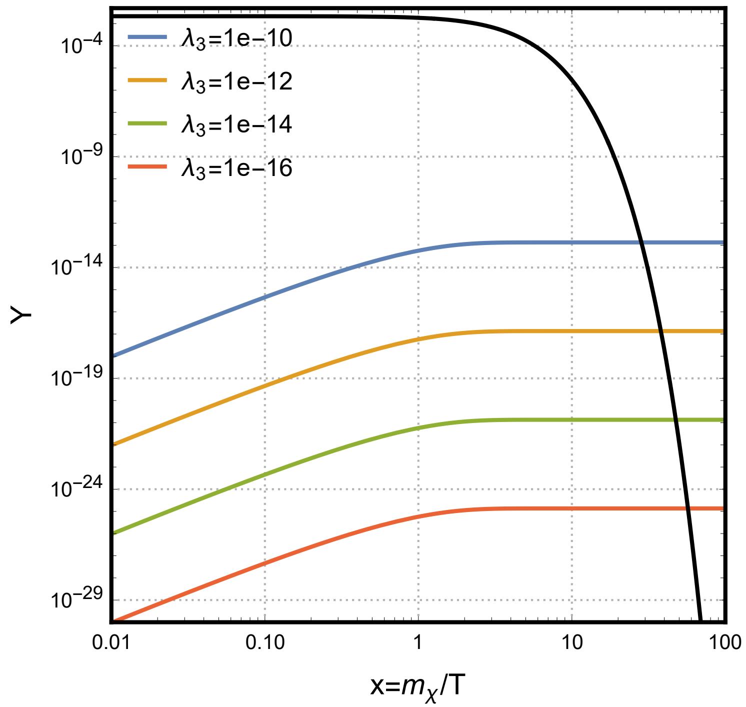

At temperatures lower than the dark matter mass, the bath no longer has enough energy to produce dark matter. At this point, the amount of dark matter has "frozen-in," there are no other ways to produce more dark matter.

Mechanisms of DM generation - pandemic

This is a mechanism that complements freeze-in and freeze-out production in a generic way, opening new parameter space to explain the observed DM abundance.

To make this work we need at least two DM particles (χ, ψ). ψ is already in thermal equilibrium with the SM bath in the early universe. χ has a small initial value abundance created by freeze-in. Interaction between ψ and χ leads to an exponential growth of χ that shuts down at some point.

In this scenario we extend the SM with two real singlet scalar fields χ, ψ that are odd under Z_2 and all SM particles are even. The most general renormalisable Lagrangian is

$$
\begin{aligned}
\mathcal{L}_{\text{scalar,int}} = &- m_{11}^2 \Phi_1^\dagger \Phi_1 + m_{22}^2 \Phi_2^2 + m_{33}^2 \Phi_3^2 + m_{23} \Phi_2 \Phi_3 \\
&+ \lambda_1 (\Phi^\dagger \Phi)^2 + \lambda_2 \Phi_2^4 + \lambda_3 \Phi_3^4 + \lambda_{12} (\Phi_1^\dagger \Phi_1) \Phi_2^2 + \lambda_{13} (\Phi_1^\dagger \Phi_1) \Phi_3^2 \\
&+ \lambda_{23} \Phi_2^2 \Phi_3^2 + \lambda_{123} (\Phi_1^\dagger \Phi_1) \Phi_2 \Phi_3 + \lambda_{223} \Phi_2^3 \Phi_3 + \lambda_{332} \Phi_3^3 \Phi_2 .
\end{aligned}
$$

Here the terms which leads to freeze-in and exponential growth are highlighted.

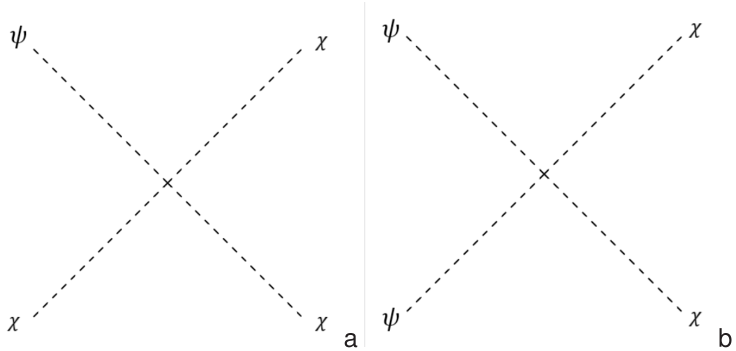

Figure: Feynman diagram of (a) the exponential growth process and (b) of the freeze-in process

$$
\frac{\mathrm{d}Y_\chi}{\mathrm{d}t} = -\sqrt{\frac{\pi}{45G}} \frac{g_*^{1/2} m_\psi}{x^2} \left(\langle \sigma v \rangle_{\text{tr}} Y_\psi^{\text{eq}} Y_\chi - \langle \sigma v \rangle_{\text{fi}} (Y_\psi^{\text{eq}})^2 \right).
$$

This is an x!

Mechanisms of DM generation - pandemic

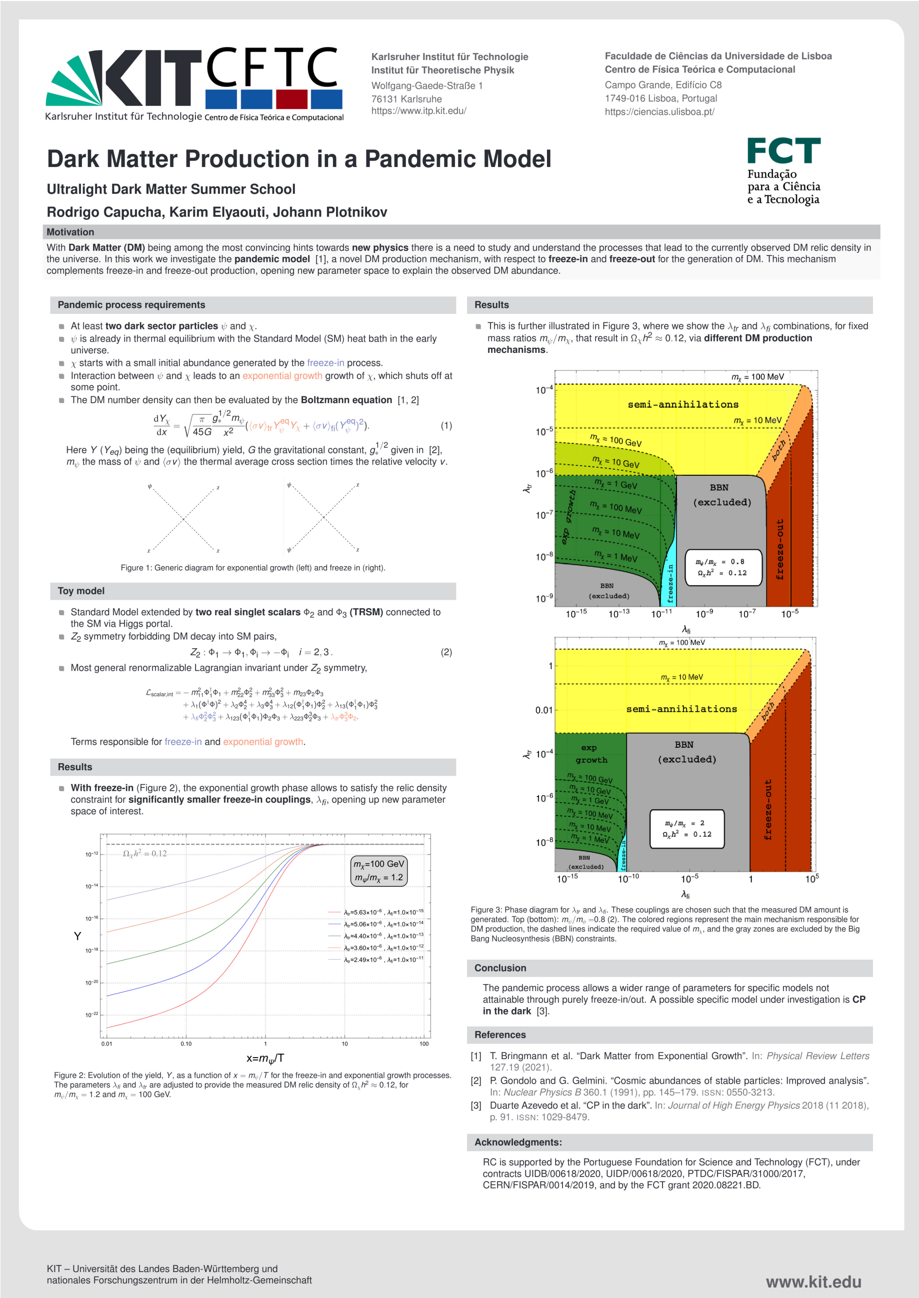

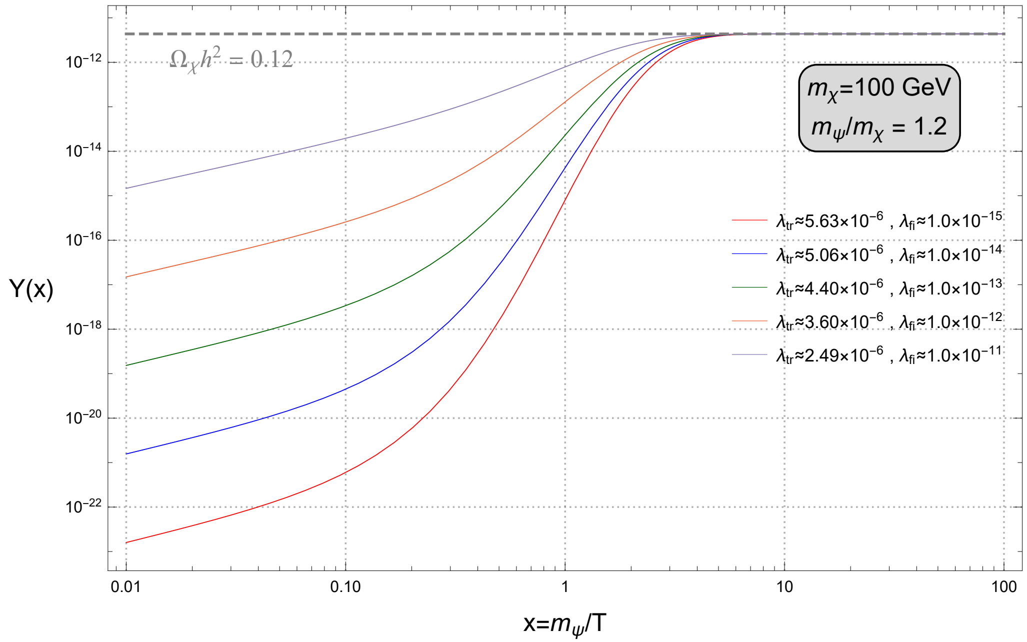

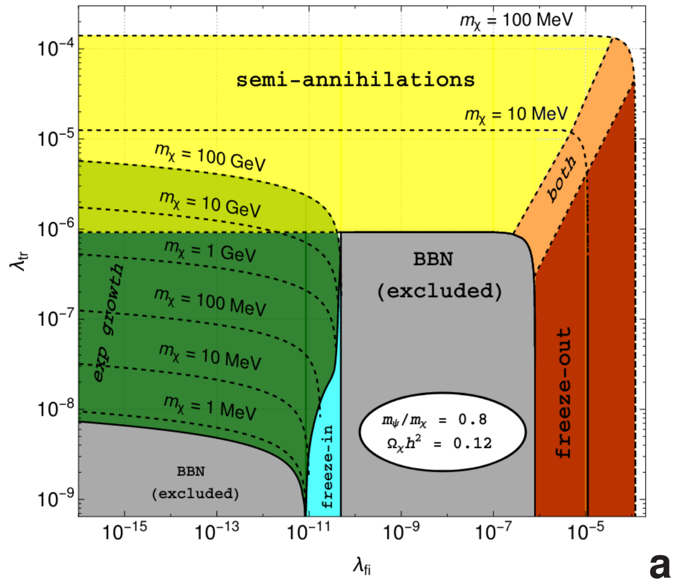

a

Mechanisms of DM generation - freeze-out

$$\mathcal{M} = \bar{u}(k_2)\,\frac{-im_f}{v_H}\,v(k_1)\,\frac{-i}{(k_1+k_2)^2 - m_H^2 + im_H\Gamma_H}\,(-2i\lambda_3 v_H)$$

$$\begin{aligned}
\sum_{\text{spin}} |\mathcal{M}|^2 &= 4\lambda_3^2 m_f^2 \left(\sum_{\text{spin}} v(k_1)\bar{v}(k_1)\right)\left(\sum_{\text{spin}} u(k_2)\bar{u}(k_2)\right)\frac{1}{\left|(k_1+k_2)^2 - m_H^2 + im_H\Gamma_H\right|^2} \\
&= 4\lambda_3^2 m_f^2 \;\mathrm{Tr}\left[(\not{k}_1 - m_f \mathbb{1})\,(\not{k}_2 + m_f \mathbb{1})\right]\frac{1}{\left[(k_1+k_2)^2 - m_H^2\right]^2 + m_H^2\Gamma_H^2} \\
&= 4\lambda_3^2 m_f^2 \; 4\left[k_1 k_2 - m_f^2\right]\frac{1}{\left[(k_1+k_2)^2 - m_H^2\right]^2 + m_H^2\Gamma_H^2} \\
&= 8\lambda_3^2 m_f^2 \,\frac{(k_1+k_2)^2 - 4m_f^2}{\left[(k_1+k_2)^2 - m_H^2\right]^2 + m_H^2\Gamma_H^2}\,.
\end{aligned}$$

$$\overline{\sum_{\text{spin,color}} |\mathcal{M}|^2} = N_c\; 8\lambda_3^2 m_b^2\,\frac{s - 4m_b^2}{\left(s - m_H^2\right)^2 + m_H^2\Gamma_H^2}$$

$$\begin{aligned}
\sigma(SS \to b\bar{b}) &= \frac{1}{16\pi s}\sqrt{\frac{1 - 4m_b^2/s}{1 - 4m_S^2/s}}\;\overline{\sum |\mathcal{M}|^2} \\
&= \frac{N_c}{2\pi\sqrt{s}}\,\lambda_3^2 m_b^2\sqrt{\frac{1 - 4m_b^2/s}{s - 4m_S^2}}\;\frac{s - 4m_b^2}{\left(s - m_H^2\right)^2 + m_H^2\Gamma_H^2}
\end{aligned}$$

$$\begin{aligned}
\langle\sigma v\rangle\Big|_{SS\to b\bar{b}} \equiv \sigma v\Big|_{SS\to b\bar{b}} &\overset{\text{Eq.(3.19)}}{=} v\,\frac{N_c\lambda_3^2 m_b^2}{2\pi\sqrt{s}}\,\frac{\sqrt{1 - 4m_b^2/s}}{m_S v}\,\frac{s - 4m_b^2}{\left(s - m_H^2\right)^2 + m_H^2\Gamma_H^2} \\
&\overset{\text{threshold}}{=} \frac{N_c\lambda_3^2 m_b^2}{4\pi m_S^2}\sqrt{1 - \frac{m_b^2}{m_S^2}}\;\frac{4m_S^2 - 4m_b^2}{\left(4m_S^2 - m_H^2\right)^2 + m_H^2\Gamma_H^2} \\
&\overset{m_S \gg m_b}{=} \frac{N_c\lambda_3^2 m_b^2}{\pi}\,\frac{1}{\left(4m_S^2 - m_H^2\right)^2 + m_H^2\Gamma_H^2}\,.
\end{aligned}$$

DM - scalar vs. vector

Scalar vs. vector

PARTICLE CONTENT

VDM: SM + vector dark matter + new scalar

SDM: SM + scalar dark matter + new scalar

INDEPENDENT PARAMETERS

$$m_{DM};\ \sin\alpha;\ m_2;\ v_S$$

- m_{DM} → Mass of the DM particle
- $\sin\alpha$ → Mixing angle between doublet and singlet (real)
- m_2 → Mass of the second scalar
- v_S → Singlet VEV

Parameter	Range
SM-Higgs—m_1	125.09 GeV
Second Higgs—m_2	[1,1000] GeV
DM—$m_{\rm DM}$	[1,1000] GeV
Singlet VEV—v_s	$[1,10^7]$ GeV
Mixing angle—α	$[-\frac{\pi}{4},\frac{\pi}{4}]$

There is obviously a 125 GeV Higgs (other scalar can be lighter and heavier).

Experimental and theoretical constraints to be discussed next

Scalar vs. vector

Theoretical and collider constraints:

Points generated with ScannerS requiring

- absolute minimum
- boundedness from below
- that perturbative unitarity holds
- S,T and U

Signal strength: gives a constraint on cosα

Searches: BR of Higgs to invisible below 24%

Searches: for extra scalars imposed via HiggsBounds which gives a bound that is a function of the new scalar mass and cosα

Scalar vs. vector

Cosmological constraints:

DM abundance: we require

$$(\Omega h^2)_{DM} < 0.1186$$ [Calculated with MicroOmegas]

or to be in the 5σ allowed interval from the Planck collaboration measurement

$$(\Omega h^2)_{DM}^{obs} = 0.1186 \pm 0.0020$$

Direct detection: we apply the latest XENON1T bounds

$$\sigma_{DM,N}^{eff} = f_{DM}\,\sigma_{DM,N} \quad \text{with} \quad f_{DM} = \frac{(\Omega h^2)_{DM}}{(\Omega h^2)_{DM}^{obs}}$$ [Fraction contributing to the scattering]

Indirect detection: for the DM range of interest, the Fermi-LAT upper bound on the dark matter annihilation from dwarfs is the most stringent. We use the Fermi-LAT bound on bb.

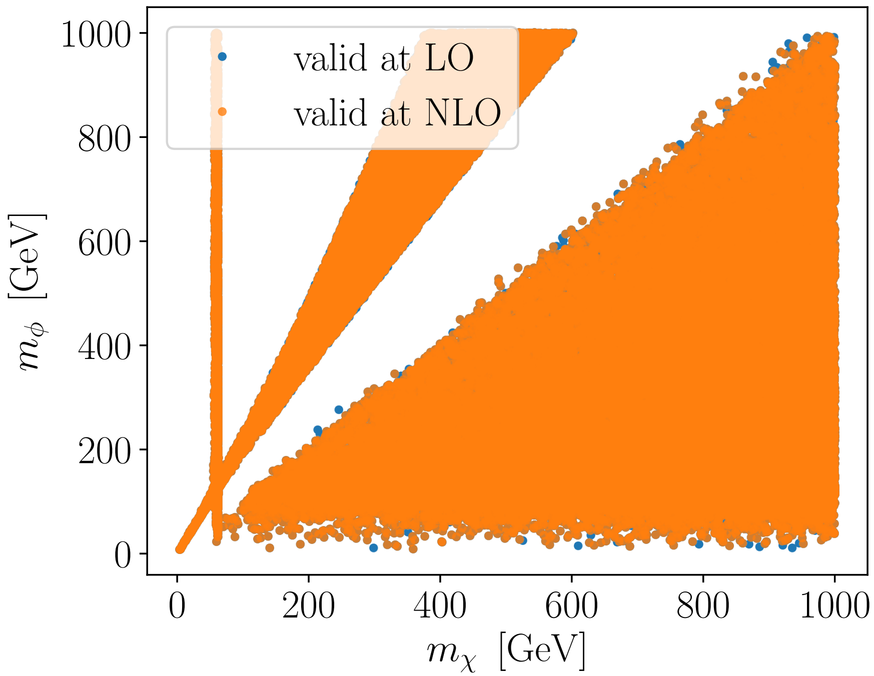
valid at LO
valid at NLO
m_ϕ [GeV]
m_χ [GeV]
1000
800
600
400
200
0

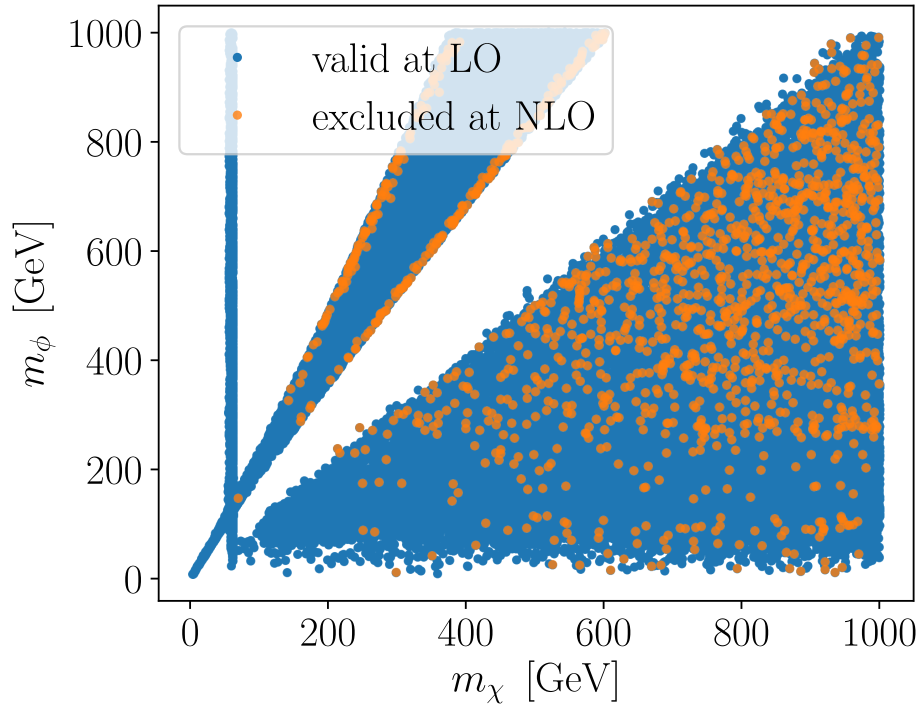
valid at LO
excluded at NLO
m_ϕ [GeV]
m_χ [GeV]
1000
800
600
400
200
0

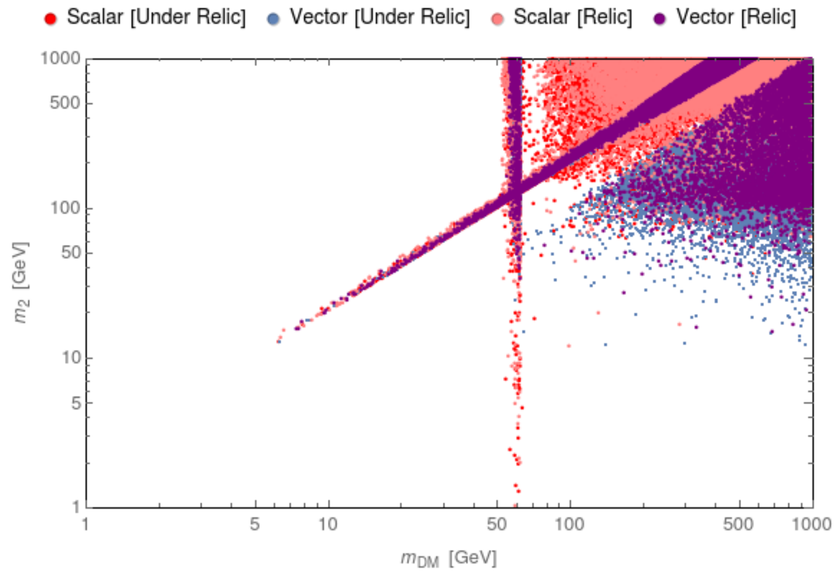
Scalar [Under Relic]
Vector [Under Relic]
Scalar [Relic]
Vector [Relic]
m_2 [GeV]
m_{DM} [GeV]
1000
500
100
50
10
5
1

Indirect detection

Indirect detection

There are many on-going experiments with the goal of detecting the products of DM annihilation in our Galaxy, or beyond.

We assume that DM annihilation is strongly suppressed after thermal freeze-out. However, it can still occur today and the chances of discovery can be maximised by searching in regions of very high DM density.

For most extensions of the SM, DM can annihilate to most of the SM particles.

We will just focus on photon final states. Depending on the model, DM can annihilate directly into a pair of photons, or into other SM states that then produce photons. The gamma-rays propagate essentially unperturbed, and can be detected by a satellite or ground-based telescope on Earth.

Let us consider that there are multiple DM annihilation channels, each with velocity-averaged cross section $\langle \sigma_i v \rangle$. The annihilation rate per particle is

$$\sum_i \frac{\rho\left[r(\ell,\psi)\right]}{m_\chi} \times \langle \sigma_i v \rangle$$

where r is the radial distance between the annihilation event and the Galactic Center—it is a function of the line-of-sight (l.o.s.) distance, l, which is oriented an angle ψ away from the Galactic plane.

Indirect detection

The total annihilation rate in the volume dV = l^2 dl dΩ is obtained by multiplying the previous equation by the total number of particles in the volume

$$\left(\sum_i \frac{\rho\left[r(\ell,\psi)\right]}{m_\chi}\langle\sigma_i v\rangle\right)\times\left(\frac{\rho\left[r(\ell,\psi)\right]}{2\,m_\chi}\,dV\right)$$

Factor of 2 because we need to DM particles to annihilate

The photon flux is the annihilation rate multiplied by dN_i/dE_γ, that is, the number of photons at a given energy E_γ produced in the i^{th} annihilation channel. The differential photon flux $d\Phi/dE_\gamma$ in the observational volume oriented in the direction ψ is

$$\frac{d\Phi}{dE_\gamma}(E_\gamma,\psi)=\frac{1}{4\pi}\int_{\Delta\Omega}d\Omega\int_{\mathrm{l.o.s.}}d\ell\,\rho\left[r(\ell,\psi)\right]^2\sum_i\frac{\langle\sigma_i v\rangle}{2m_\chi^2}\frac{dN_i}{dE_\gamma}$$

All the astrophysical uncertainties in the determination of the flux are absorbed by the J-factor

$$J=\frac{1}{\Delta\Omega}\int d\Omega\int_{\mathrm{l.o.s.}}d\ell\,\rho\left[r(\ell,\psi)\right]^2$$

The larger the J-factor, the more interesting the astrophysical target is for DM annihilation. The J-factors for dwarf galaxies are roughly J ~ 10^{19-20} GeV^2/cm^5. For our nearest neighbour, the Andromeda galaxy, J ~ 10^{20} GeV^2/cm^5. For our own Galactic Center, J ~ 10^{22-25} GeV^2/cm^5 (10^{22-24}) within 0.1°(1°).

The final state particles are stable leptons or protons propagating large distances in the Universe. While the leptons or protons can come from many sources, the anti-particles appear much less frequently. One key experimental task in many indirect dark matter searches is therefore the ability to measure the charge of a lepton, typically with the help of a magnetic field. For example, we can study the energy dependence of the antiproton–proton ratio or the

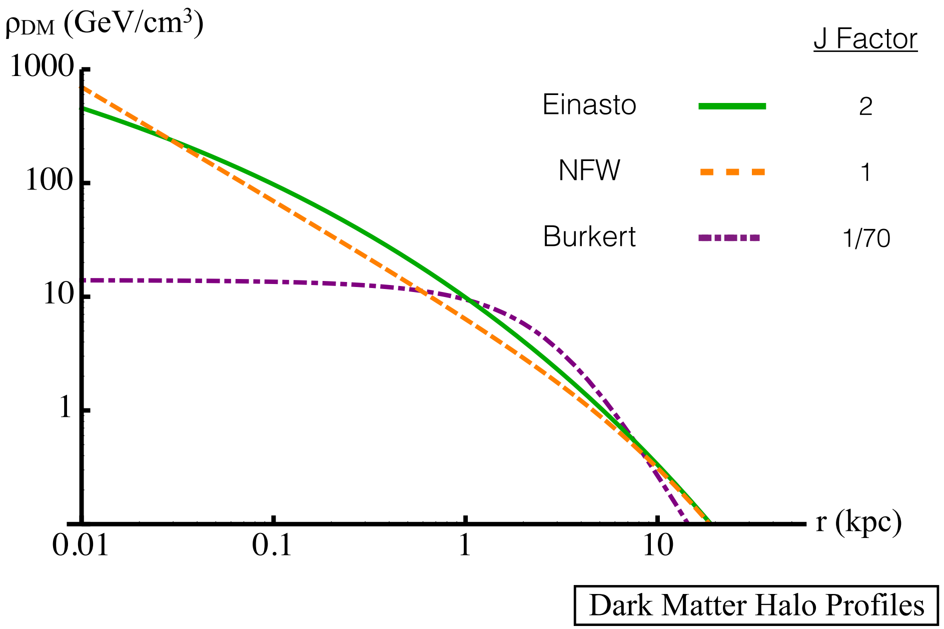

Figure 14: Dark matter galactic halo profiles, including standard Einasto and NFW profiles along with a Burkert profile with a 3 kpc core. J factors are obtained assuming a spherical dark matter distribution and integrating over the radius from the galactic center from $r \simeq 0.05$ to 0.15 kpc. J factors are normalized so that $J(\rho_{\text{NFW}}) = 1$. Figure from Ref.[12]

Indirect detection

However, when we choose a good target, there is a balance between the size of the J-factor and the potential backgrounds that has to be taken into account.

As an example, dwarf galaxies are DM-dominated and therefore some of the cleanest systems to search for DM because they contain very few stars and little gas. In contrast, a signal from the center of the Galaxy, while enhanced due to the DM density and proximity, has to contend with large systematic uncertainties on the astrophysical backgrounds.

The particle physics input to the flux is the factor (in most cases the velocity-averaged cross section can be pulled out of the integral)

$$\frac{<\sigma v>_{\chi\chi}}{m_\chi^2}\frac{dN}{dE_\gamma}$$

The kinematics of the annihilation event determine the basic properties of the photon energy spectrum. Consider, first, the case where the DM annihilates directly into one or two photons: $\chi\chi \rightarrow \gamma X$, where X = γ, Z, H or some other neutral state. In the non-relativistic limit, energy conservation gives

$$2\,m_\chi = E_\gamma + \sqrt{E_\gamma^2 + m_X^2} \longrightarrow E_\gamma \approx m_\chi\left(1 - \frac{m_X^2}{4m_\chi^2}\right)$$

E_γ is the energy of the outgoing photon in the CM frame and m_X is the mass of the X state.

The $\gamma\gamma$ final state results in a monochromatic energy line at the DM mass. For a γZ final state, the gamma line is still monochromatic, but is shifted to lower energies.

Indirect detection

Blue lines - energy spectrum for a γγ final state where the measured energy resolution is ΔE/E = 0.15 (solid) or 0.02 (dotted). The observation of such a gamma-ray 'line' would be spectacular evidence for DM annihilation. However, the production of a pair of gamma-rays is typically loop-suppressed (and therefore sub-dominant) in many theories.

Red lines - how the spectrum changes if photons are radiated off of virtual charged particles in the loop.

Green lines - illustrate the box spectrum, which arises when the DM annihilates to a new state φ (e.g., χχ → φφ) that then decays to a photon pair (φ → γγ).

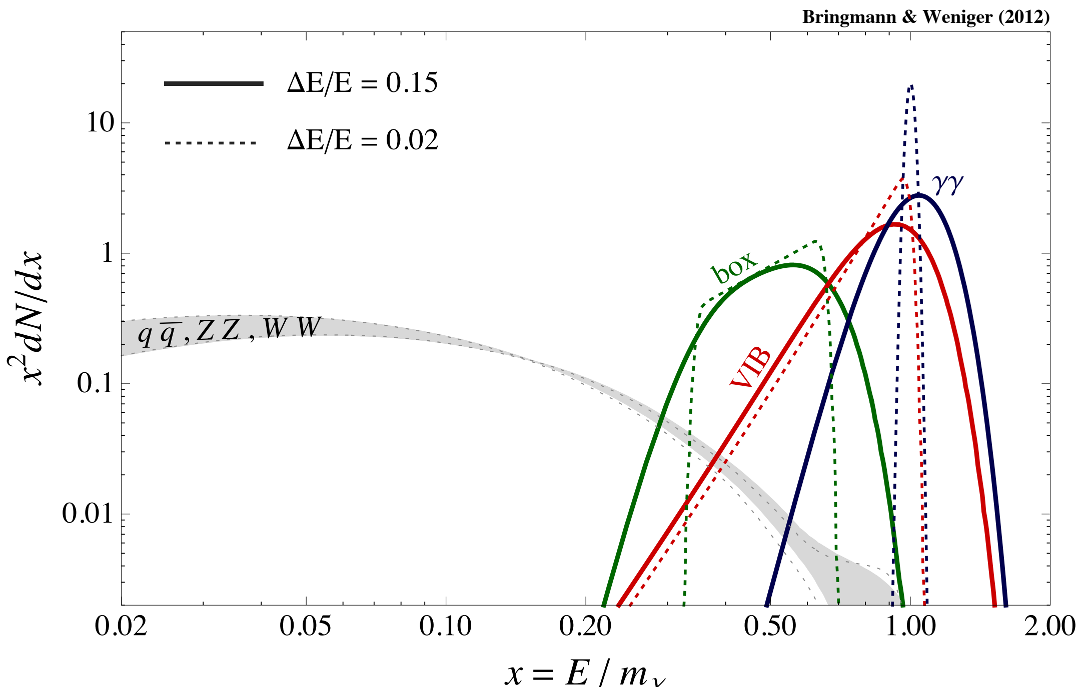

Figure 10: Illustration of the photon energy spectrum for the $\gamma\gamma$ final state without (blue) and with (red) virtual internal bremsstrahlung. The box spectrum (green) can be produced if the DM annihilates to a new state, that then decays to photons, as described in the text. The dotted versus solid lines compare two separate energy resolutions: $\Delta E/E = 0.02$ and 0.15, respectively. The spectrum for photons resulting from the annihilation into gauge bosons and quarks is shown by the gray band. Figure from [96].

Indirect detection

Another possibility is that the DM annihilates to leptons, gauge bosons, or quarks, which may produce <u>secondary photons</u> either through final-state radiation or in the shower of their decay products. The photon energy spectrum dN/dE_γ depends on the exact details of the final-state radiation, and must be determined with Monte Carlo tools like Pythia.

In the case of secondary photon production, the energy spectrum does not have a very distinctive shape, and one must search for a continuum excess over the background. The grey band in shows an example of the spectrum for annihilation to quarks or gauge bosons.

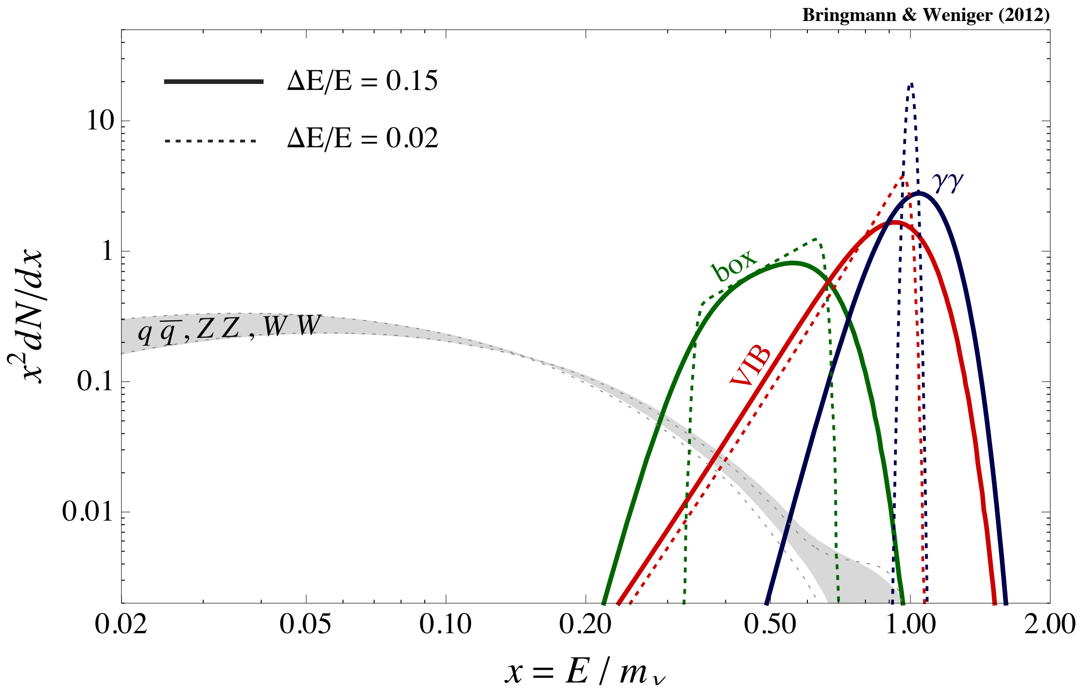

Figure 10: Illustration of the photon energy spectrum for the $\gamma\gamma$ final state without (blue) and with (red) virtual internal bremsstrahlung. The box spectrum (green) can be produced if the DM annihilates to a new state, that then decays to photons, as described in the text. The dotted versus solid lines compare two separate energy resolutions: $\Delta E/E = 0.02$ and 0.15, respectively. The spectrum for photons resulting from the annihilation into gauge bosons and quarks is shown by the gray band. Figure from [96].

Indirect detection

The details of the annihilation mechanism are in the velocity-averaged cross section ⟨σv⟩. This cross section is the same in many simple models as what appears in the relic density calculation.

In addition, we automatically have an interesting target scale for the cross section: 3×10^{-26} cm^3 s^{-1}. This regime was probed by the best gamma-ray observatories. For example, the Fermi Large Area Telescope has searched for signals of DM annihilation in the Milky Way's dwarf galaxies.

Figure show the results for DM annihilation (from FermiLAT) to bb (left) and tau tau (right)

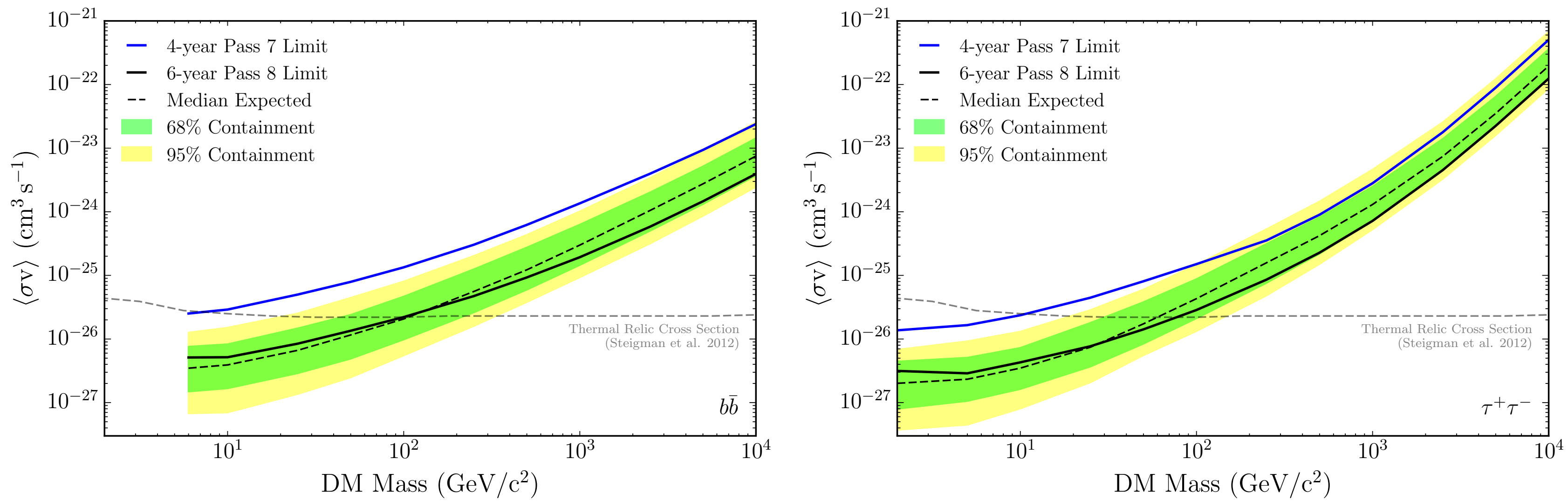

Figure 11: *Fermi* LAT limits on DM annihilation into $b\bar{b}$ (left) and $\tau^+\tau^-$ (right) final states. The dashed black line is the expected bound with 68% and 95% contours shown in green and yellow, respectively. The solid black line is the observation with six-year Pass 8 data. Figure from [99].

Indirect detection